Science of Sintering, **50** (2018) 357-369

doi: https://doi.org/10.2298/SOS1803357E

UDK: 692.533.1; 546.62

Structural, Morphological and Electrical Properties of Alumina/YAG Composites as Solid Electrolyte for IT – SOFC

Adela Egelja[1], Snežana Pašalić[1], Vladimir Dodevski[1], Milan Kragović[1], Ivana Stojković-Simatović[2], Željko Radovanović[3], Marija Stojmenović[1*)]

[1]Institute of Nuclear Sciences "Vinča", University of Belgrade, Mike Petrovića–Alasa 12–14, 11001 Belgrade, Serbia

[2]Faculty of Physical Chemistry, University of Belgrade, Studentski trg 12, 11000 Belgrade, Serbia

[3]Innovation Center of the Faculty of Technology and Metallurgy, University of Belgrade, Karnegijeva 4, 11070 Belgrade, Serbia

Abstract:

Alumina/YAG composites (AYX_t) with high relative density (99.2 %TD) were successfully obtained by mixing commercial alumina powder with different volume fractions of yttrium aluminium garnet ($Y_3Al_5O_{12}$-YAG; 7, 14, 21 and 28). YAG was synthetized by nitrate glycine reaction in the form of precursor powder. Polycrystalline YAG powder was obtained by calcination at 950 °C for 2 h. Additionally, obtained compositions were characterized by XRD, SEM, EDX and electrochemical impedance spectroscopy. By XRPD analysis was found that the particle size of YAG powders lies in the nanometric range (being lower than 35 nm). By SEM microphotographs of composites were confirmed the formation of a conductive path consisting from mutually interconnected YAG particles. This was confirmed by the electrochemical impedance spectroscopy. The highest electrical conductivity of grain (κ_g) and grain boundary (κ_{gb}) at 700 ºC amounted to 2.22×10^{-2} $\Omega^{-1}cm^{-1}$and 9.44×10^{-3} $\Omega^{-1}cm^{-1}$, respectively, was measured in the composite containing 21 vol% of YAG.

Keywords: *Al_2O_3-YAG; Composites; Electrical conductivity.*

1. Introduction

In the past few decades, unquestionable advantage was given to develop technologies for the appropriate industrial production of solid oxide fuel cells (SOFCs) [1, 2]. Development of strong and sTab. high-temperature structural ceramics for SOFCs is nowadays one of the very interesting research topics [1, 2]. In the past few years the research was focused to reduce the operating temperature in the intermediate area (500-700 °C) and formation intermediate temperature solid oxide fuel cells (IT-SOFC) with high energy efficiency [3, 4]. In order to enhance the performance of IT-SOFCs such as energy efficiency, it is important to investigate behavior of electrolytes [3, 4]. Yttrium stabilized zirconia (YSZ) [5], as well as pure and doped ceria (IV) oxide (CeO_2) [3, 4], are the most commonly used as electrolytes for SOFC. However, YSZ operates at temperatures above 1000 °C, and the cost is high due to the high amount of zirconia. On the other hand, CeO_2 operates at temperatures below 700 °C, but the cost is also high because of the considerable amount of expensive CeO_2.

From this point of view, the combination of alumina (Al_2O_3) and yttrium aluminum garnet ($Y_3Al_5O_{12}$-YAG) in the form of composites with the second phase gives the possibility

*) **Corresponding author:** mpusevac@vinca.rs

of obtaining a structural material with promising properties [6-8]. Namely, Al_2O_3 represents one of the most popular oxide materials with good mechanical properties, whereas YAG is very sTab. in contact with Al_2O_3 up to 1700 °C [6-8] and has similar coefficients of thermal expansion as alumina.

Application of the electrical conductivity of composites based on Al_2O_3 can be reinforced by the addition of conductive or semiconductive phases such as YAG. YAG is a potential reinforcement because of its excellent creep resistance, thus creating alumina-YAG as an attractive composite material [6-8]. There are different routes and techniques which have been used to prepare powders for densification in the Al_2O_3/YAG system [9, 10]. Characteristics of starting powders, such as sinterability, purity, homogeneity and particle size have a huge impact on the quality of the sintered composite [9, 10]. In other words, powders synthesized by different methods have different properties, i.e. sintering behavior. Alumina and YAG powders can be simply mixed by mechanical mixing. The mixing of powders is a very important procedure because of the green structure, since pore size distribution plays an important role in achieving high density of ceramics [6, 11]. However, this method requires extensive mechanical ball milling which may introduce impurities [6-11]. Water solution mixing is a more appropriate technique to obtain a uniform distribution of YAG particles in the alumina matrix [7-11]. Thus, in this case the functional properties such as the composition of powder mixtures with different volume fraction of the second phase (YAG), the parameters of the composite structure (the size of alumina matrix grains, and the size and distribution of YAG), as well as the content of impurities present very important factors. These features, as well as much cheaper production, created YAG-aluminum as an attractive composite material, which, as a semiconductor ceramic, might be of special interest for industrial application.

Taking into account all above-mentioned reasons, although many electrolytes for SOFC were ready for commercialization, the aim of this work was to prepare composites based on Al_2O_3 with different volume fractions of YAG (7, 14, 21, 28) with improved electrical conductivity. The characterization of the obtained composites was performed from the point of view of their structure, morphology and electrical properties. Particular attention was paid to improve starting material in the form of a precursor, such as YAG, and its impact on structure, morphology and electrical properties of obtained Al_2O_3/YAG composites.

2. Experimental procedure

2.1. Synthesis of powders

Preparation of composites was performed in three phases. The starting procedure consisted of synthesizing 100 g of YAG by the glycine-nitrate combustion method, which is relatively low cost method with fast heating rates, short reaction times, high composition homogeneity and high energy efficiency [13]. In the second phase Al_2O_3/YAG powders (AYX_p) were synthesized with different content of YAG (X is 7, 14, 21 and 28 vol.% of YAG in the Al_2O_3 matrix; p denotes powder). In the third phase Al_2O_3/YAG composites were sintered at 1550 °C during different time (AYX_t; t is duration of sintering time).

Glycine-nitrate method was used for synthesis of YAG powder in the form of precursor ($Y_3Al_5O_{12}$). The starting chemicals were Y-nitrate ($Y(NO_3)_3{\cdot}6H_2O$, Aldrich, USA, 99.9 %), Al-nitrate ($Al(NO_3)_3{\cdot}9H_2O$, Aldrich, USA, 99.9%) and glycine (Fischer Scientific, USA, 99.999 %). Preparation of precursor YAG powder was performed according to the following reaction:

$$3Y(NO_3)_3{\cdot}6H_2O + 5Al((NO_3)_3{\cdot}9H_2O + C_2H_5NO_2 \rightarrow Y_3Al_5O_{12} + 2CO_2 + 25NO_2 + 65{,}5H_2O + 2{,}75O_2$$

Firstly, all reactants were dissolved in distilled water and then poured in a stainless-steel reactor. It was heated gently until the viscous liquid fumed and combustion reaction was set in, resulting in the production of gaseous bubbles without violent bursting. Reaction was carried out at 500 °C for about 1 h. Obtained powder was than calcined at 800 °C for 2 h to remove NO_x gases. However, this temperature was not high enough for forming YAG crystallization and therefore material was subsequently calcined at 950 °C for 2 h.

Four composites with different powder compositions, i.e. AYX (X is 7, 14, 21 and 28 vol.% of YAG in the Al_2O_3 matrix) were prepared by homogenization of YAG powder with the high purity Al_2O_3 powder (CT3000-SG, Alcoa, 99.92 %) and with addition of 5 wt.% (polyethylene glycol-PEG; Aldrich, USA) as a binder. Pure alumina (AY0) and pure YAG (A0Y) were also prepared for comparison. These powder mixtures were homogenized for 24 h using alumina balls of graded sizes and with small amount of distilled water to get a slurry texture. Subsequently, composites were dried at 90 °C for 24 h in the air. The agglomerated powders were then crushed and sieved. Cylindrical samples of 9.3 mm diameter were uniaxially compacted at 100 MPa and isostatically repressed at 300 MPa. The binder from samples was removed by a very slow air heating up to 630 °C with heating rate of 0.5 °C/min. During the heating process samples were held for 1 h and 30 at 160 °C and 220 °C, respectively. Afterwards, the samples were sintered at 1550 °C for 2, 4, 6 and 8 h. Densities of all obtained composites (AYX_t; t is sintering time duration) were measured by the Archimedes' method in distilled water and referred to the theoretical density (TD) using 3.97 g/cm^3 for alumina [9] and 4.56 g/cm^3 for YAG [9]. Densified composites were characterized using X-ray diffraction (XRD), scanning electron microscopy (SEM), energy dispersive spectroscopy (EDS) and complex impedance methods.

2.2. Sample characterization

The crystalline phases were identified by X-ray powder diffraction (XRD) analysis using a Ultima IV Rigaku diffractometer, equipped by Cu $K\alpha_{1,2}$ radiation, with generator voltage 40.0 kV and generator current 40.0 mA. The range of 10–80° 2θ was used for all powders in a continuous scan mode with a scanning step size of 0.02° and at a scan rate of 2°/min. Before measurement, the angular correction was performed by means of a high-quality Si standard.

The microstructural analysis of powder composites and sintered composites were investigated by scanning electron microscope (SEM) model FE-SEM Jeol JSM 6330F (Japan). Prior to examination the surface was coated with a thin layer of gold. The images were recorded in SEI mode at a magnification ×50 kx with the accelerating voltage of 4 kV. Average grain sizes were measured from SEM micrographs. The chemical compositions of the sintered composites were analyzed by energy dispersive spectrometer (EDS) Isis 3.2, with a SiLi X−ray detector (Oxford Instruments).

The electrical properties were measured by electrochemical impedance spectroscopy (EIS), in the frequency range 1 Hz – 0.1 MHz, using Gamry 750 ZRA potentiostat/galvanostat and EIS 300 Impedance Software. The measurements were conducted in an air, in the temperature range 500-700 ºC, with an increment of 50 ºC. The amplitude of the applied sinusoidal voltage signal was 20 mV. Thin layer of high conductivity silver paste was applied onto both sides of the sample pellets in order to provide good electrical contact between electrolyte and electrodes. The samples were placed between silver plates in a ceramic holder, which was heated in a vertical oven. A Pt–Rh thermocouple located just below the bottom of silver plate was used for temperature monitoring. The impedance data were used to estimate appropriate equivalent circuit by software Z–View2 (version 2.6 demo). The resistance values were determined from the impedance diagrams recorded at various temperatures. The specific conductance was calculated from the resistance data using dimensions of the sample pellets.

3. Results and discussion

3.1. Structural properties of calcined and sintered samples

Fig 1. shows the XRD pattern of pure commercial alumina (ICDD Al_2O_3 01-075-1862). Crystalline size was calculated from Scherrer formula from XRD peaks. Calculated value is 29.7 nm and lattice parameters are a (Å) = 4.762, b (Å) = 4.762, c (Å) = 12.997.

Fig. 2a shows the XRD patterns of synthesized YAG powder in the form of precursor treated by heating at 700 °C, 800 °C and 920 °C. The peaks in Fig. 2a indicate that at 700 °C and 800 °C precursor YAG powder is still amorphous (ICDD: Y_2O_3 01-071-0099; Al_2O_3 01-088-0826) and consists of properly mixed aluminum, yttrium and oxygen atoms. By further heating up to 880 °C the precursor YAG powder was still amorphous. However, during heating at 920 °C the composition was a mixture of hexagonal YAP (YAH) and cubic YAG [12] appeared, which was confirmed by XRD result (Fig. 2a). This intermediate structure transforms into crystalline YAG phase owing to increased atom mobility and reactivity at higher temperatures. Based on that, the crystallization and transformation of pure cubic YAG occurred during the calcinations process at 950 °C without traces of the undecomposed nitrates, as it is shown in Fig. 1b (ICDD: YAG 01-070-7794).

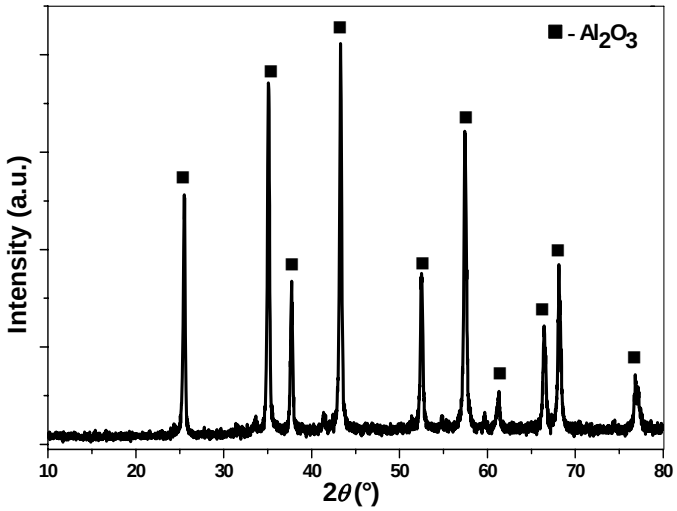

Fig. 1. XRD pattern of pure alumina.

Crystallite size was calculated from Scherrer formula $D_{hkl}=k\alpha/(\beta \cos\theta)$ from XRD peaks of YAG calcinated at five different temperatures (Fig. 2b). Values were presented in Tab. I and it may be noted that crystals become larger with increase in calcination temperature. Based on the literature data [13] it is assumed that the YAG powder with smallest crystalline size is much more sinterable with Al_2O_3 particles. Namely, literature data [13, 14] have shown that although pinning efficiency of large particles of second phase was high, low pinning efficiency of single nanoparticles was only partially compensated by their number. Individual nanoparticles were swallowed by growing grains and were often located in intragranular positions [13, 14]. However, the nanoparticles of the second phase often form larger agglomerates with high pinning efficiency along grain boundaries creating a conductive path [13, 14]. This continuous conductive path consists of the second phase particles in contact with each other, or separated by small gaps, will be discussed in detail in section 3.3. Thus, for this purpose the YAG powder with smallest crystalline size calcinated at 950 °C was used in the further part of the experiment.

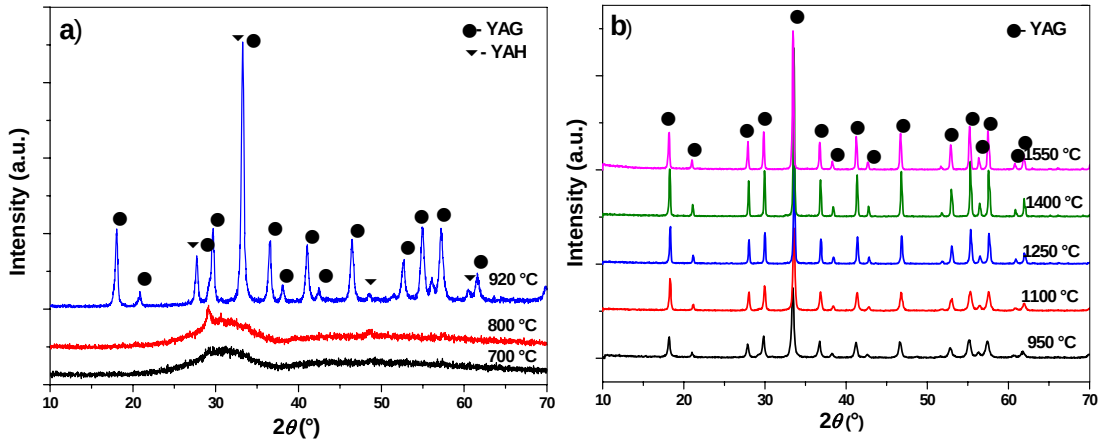

Fig. 2. XRD patterns of: a) precursor YAG powder heated at 700, 800 and 950 °C; b) XRD pattern of YAG calcined from 950 to 1550 °C

Tab. I Crystallite size of YAG powder calculated from Scherrer formula $D_{hkl}= k\alpha/(\beta \cos\theta)$.

Calcination temperature (°C)	Lattice parameter a (Å)	Crystallite size (nm)
950	12.031125	23.6
1100	12.035089	27.8
1250	12.019474	32.1
1400	12.007952	32.9
1550	12.012162	34.9

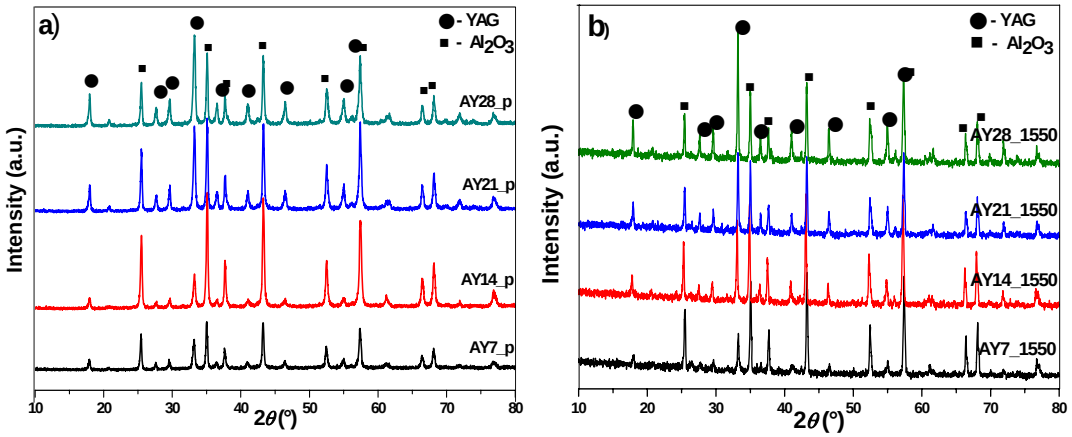

Fig. 3. XRD patterns of: a) alumina/YAG mixture powders, b) alumina/YAG composite sintered at 1550 °C.

Fig. 3 shows the XRD patterns of four mixtures of calcinated YAG powder at 950 °C and alumina powder (ICDD: YAG 01-070-7794; Al_2O_3 01-076-7775) and samples after sintering process at 1550 °C (ICDD: YAG 01-070-7794; Al_2O_3 01-076-7775). Intensity of peaks increases with the increase of sintering temperatures which is attributed to the grain growth of YAG.Lattice parameters and crystallite size of alumina/YAG mixture powders (AYX_p), and sintered composite at 1550 °C (AYX_1550; X=7, 14, 21 and 28 vol%) are presented in Tab. II.

Tab. II Lattice parameters and crystallite size of alumina/YAG mixture powders (AYX_p), and sintered composite at 1550 °C (AYX_1550; X=7, 14, 21 and 28 vol%).

	Al_2O_3			YAG	
Compositions	Lattice parameters (Å)		Crystallite size (nm)	Lattice parameter a (Å)	Crystallite size (nm)
	a	**c**			
AY0_p	4.7620	12.9970	29.7	/	/
AY0_1550	4.7631	13.0050	37.3	/	/
AY7_p	4.7530	12.9940	27.2	11.99800	15.47
AY7_1550	4.7593	12.9950	24.0	12.01000	26.72
AY14_p	4.7604	12.9946	26.8	12.03523	23.40
AY14_1550	4.7780	13.0300	19.4	12.07678	32.47
AY21_p	4.7540	13.0100	27.5	12.01100	21.64
AY21_1550	4.7600	13.0900	13.9	12.01520	28.75
AY28_p	4.7550	13.0000	25.8	12.00960	21.18
AY28_1550	4.7664	13.0200	23.9	12.03533	40.50
A0Y	/	/	/	12.031125	23.60

3.2. Densification and microstructure

Fig. 4 shows influence of volume fraction and time of sintering process on density of composites AYX_1550. A different amount of YAG strongly affects densification process and grain growth. The composite with smallest amount of YAG exhibits the highest density irrespective on sintering time and vice versa. Actually, the increase of sintering time should increase density of composites up to a certain point, since longer sintering time leads to grain growth which inhibits further densification. As Fig. 4 shows the increase of sintered time from 6 to 8 h does not lead to further densification for AY21_1550 and AY28_1550. Reduction of density also occurs due to grain growth after 8 h of sintering in composites with less amount of YAG, i.e. in AY7_1550 and AY14_1550.

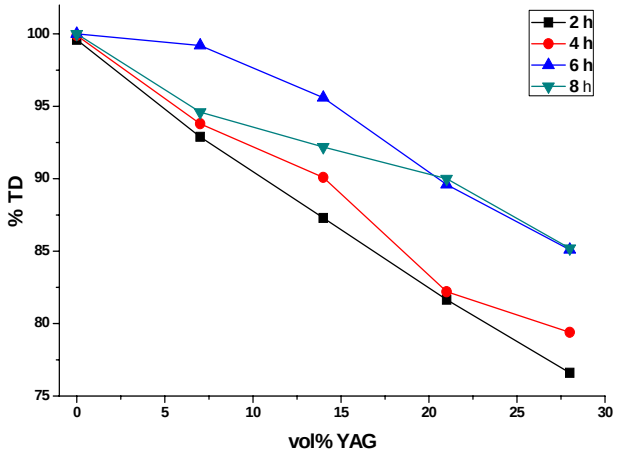

Fig. 4. Effect of volume fraction of YAG and sintered time duration on density of alumina/YAG composite.

Fig. 5a shows SEM images of four mixtures of calcinated YAG powder at 950 °C and alumina powder (AYX_p). As can be seen, the grains are irregularly shaped, weakly bonded

and with wide size distribution up to about 1 μm. Homogenization and absence of agglomerates is achieved. This is a good precondition for efficient sintering process [14-17]. Further, Fig. 5b shows SEM images of alumina/YAG composites with different volume fractions of YAG sintered at 1550 °C for 6 h (AYX_1550). Under these conditions samples obtained highest density (Tab. III). All materials possess a similar microstructure of fairly equiaxed grains and with noticeable difference in density. The white grains from the Fig. 5b were analyzed by EDS method. The EDS spectrum, given in Fig. 5c, reveals that grain is YAG as it contains Y, Al and O with atomic ratio of Al/Y=63.95/ 36.05. Based on that we postulate that YAG phase is white or at least brighter than alumina. According to SEM images (Fig. 5b) a rather homogeneous microstructure is achieved, consisting of small YAG grains embedded within the larger alumina matrix. The average grain size of YAG in all AY compositions is in the range of 0.7-2.7 μm. There is no significant change in the grain size, since all samples were sintered at the same temperature. The influence of sintering time on the grain size is negligible.

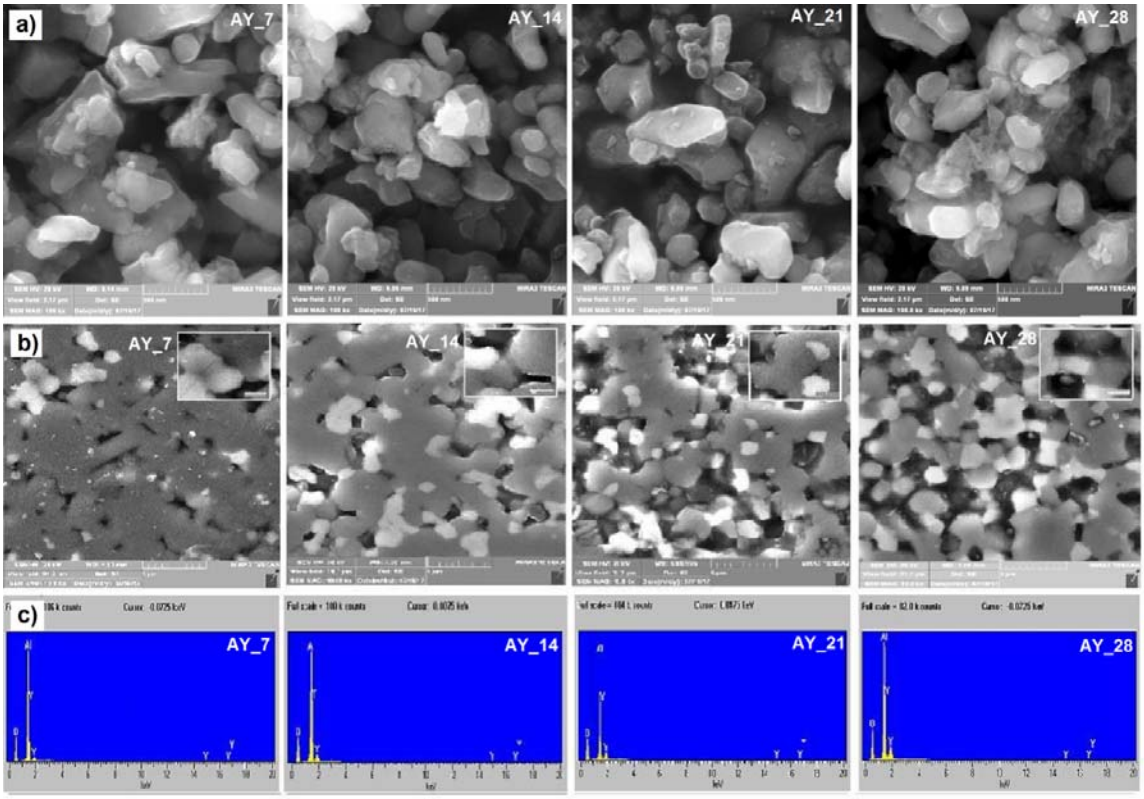

Fig. 5. SEM images of: a) powders AYX_p, and b) samples AYX_1550 sintered at 1550 °C during 6 h; and c) EDS spectra of samples AYX_1550 sintered at 1550 °C during 6 h.

Tab. III Theoretical and Archimede's densities of alumina/YAG composite at different sintering time duration.

		%TD			
		Duration of sintering time (h)			
vol% YAG	**TD (g/cm^3)**	2	4	6	8
AY7_1500	4.0113	92.9	93.8	99.2	94.6
AY14_1500	4.0526	87.3	90.1	95.6	92.2
AY21_1550	4.0939	81.6	82.2	89.9	89.6
AY28_1550	4.1352	76.7	79.5	85.1	85.2

3.3. Electrical conductivity

The grain boundaries and grain have an important role for transport properties of many materials [14]. This is especially important, since the most of atoms reside in the grain boundary or within a few atomic layers from the boundary [3-4, 14-17]. Namely, the alumina/YAG composites studied in this work were composed from Al_2O_3 matrix and YAG as the second phase, which, if is properly distributed, can create a conductive path. According to literature results [18, 19] the addition of a conductive or a semiconductive secondary phase in a non-conductive system such as Al_2O_3 can markedly influence the overall electrical conductivity of a composite with the microstructure containing percolating conductive phase. These findings also explain dependence of the conductivity and concentration of randomly dispersed second phase particles in a non-conductive matrix. Thus, it can be anticipated that the electrical conductivity of alumina/YAG composites depends on formation of a conductive path consisting of mutually interconnected YAG particles. Namely, several different studies about conductivity of YAG have been reported [20-24]. The research included electrical conductivity of undoped YAG as a function of temperature under oxidizing conditions [22], the ionic transference and conductivity measurements of $Y_3Al_5O_{12}$, $Y_3Fe_5O_{12}$ and $Y_3Ga_5O_{12}$ [23] and measurements of polycrystalline calcium doped YAG is as mixed ionic-electronic conductor, with an ionic activation energy [24]. The obtained results on the point energies for aluminium and oxygen jumps indicate that oxygen should exhibit a higher mobility in the YAG lattice than Al ions [20, 21]. However, it should be noted that in some studies it has been shown that the transport properties of polycrystalline YAG containing Al/O_3 inclusions are possibly related with the presence of Al vacancies [24]. As a very well-developed method, complex impedance method was applied to study the contribution of grains and the grain boundary of sintered ceramics in form Nyquist plot. Typical Nyquist plots of solid materials, as negative of imaginary component of impedance $-Z_{imag}$ versus real component of impedance Z_{real}, consist of three semicircles: high, intermediate and low frequency semicircles [3-4, 13, 15]. The high and intermediate frequency semicircles were ascribed to grains and grain boundary, and can be interpreted as a response of two serially connected RC circuits, which applied widely in the literature related to the sintered ceramics [3-4, 13, 15]. From this aspect, high–frequent semicircle may be attributed to a parallel connection of the grain resistance (R_g) of crystallite grains, and the geometric capacitance (C_g) of the sample. If the impedance semicircles were clearly separated, i.e. $R_gC_g << R_{gb}C_{gb}$, the values of R_g and R_{gb} may be read separately as a low–frequency intercepts of the semicircles with the real axis. By means of the frequency corresponding to the high–frequency semicircle maximum, $\omega_{max,g}$, geometric capacitance can be calculated according to the equation $\omega_{max,g}=1/R_gC_g$. The low–frequency semicircle may be attributed to the grain boundary resistance (R_{ig}) in parallel connection with the intergranular capacitance (C_{ig}). In this case, by means of the frequency which refers to the semicircle maximum, intergranular capacitance can be calculated using the well-known equation $\omega_{max,ig}=1/R_{ig}C_{ig}$. The low frequency semicircle represents the electrode process contribution, which is out of scope of this study.

In our case, the original Nyquist plots recorded in the available frequency range from 1 Hz–100 kHz is presented in Fig. 6. For potential application in IT-SOFCs the measurements electrical conductivity of alumina/YAG composites were performed in the temperature range of 500-700 ºC, with the increments of 50 ºC. As Fig. 6 shows, the spectra are composed of two semicircles which could be confidently assigned as the bulk and grain boundary responses. The values R_g and R_{gb} were estimated from the experimental cross section of obtained semicircles with real component of impedance, Z_{real} [3, 4, 13, 15]. The exact semicircles correspond to either grain or grain boundaries and appeared only when the grains are distributed uniformly. The bulk semicircle occurred in higher frequency region, and grain boundary semicircle occurred in the intermediate frequency region. However, with the increase of temperature (Fig. 6), both resistance elements (R_g and R_{gb}) decrease, which causes

an increase in ω_{max}. Consequently, the whole region of the impedance points shifts towards the low–frequency semicircle. At higher temperatures (500-700 ºC), the time constants associated with the bulk and grain boundary impedances were much lower and the semicircles, due to grain and grain boundary**,** gradually disappear and only a single semicircle can be observed (Fig. 6b).

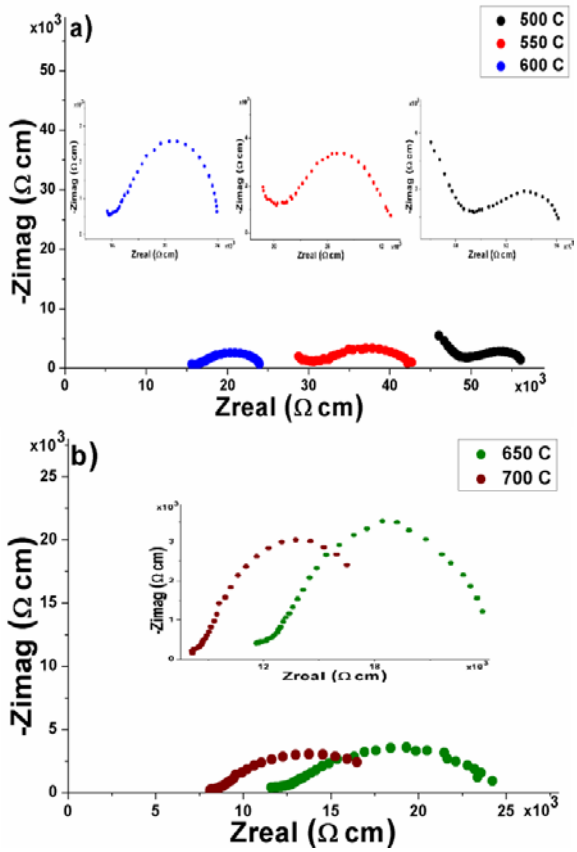

Fig. 6. Complex impedance plots of the AY21_1550 sintered sample, measured at temperatures: a) 500-600 ºC and b) 650-700 ºC, in air atmosphere. The working temperatures are indicated at each diagram

This was expected since the grain boundary semicircle is dependent on the microstructural properties of sintered sample, particularly volume fraction, distribution and grain size of the second phase. Namely, different mathematical models [13-19] calculated minimum volume fraction of secondary phase particles for creating a conductive path in Al_2O_3 matrix. The addition of various amounts of YAG particles (7-28 vol%) into the Al_2O_3 matrix, resulted in our case with processing of composites with a satisfactory electrical conductivity (Tab. IV). The highest electrical conductivity (2.22×10^{-2} $\Omega^{-1}cm^{-1}$) was measured in the composite AY21_1550, whereas the electrical conductivity of the pure Al_2O_3 was only 6.72×10^{-6} $\Omega^{-1}cm^{-1}$. Based on the presented results it can be concluded that in alumina/YAG composites electrical conductivity is conducted through a continuous network of YAG particles located inside the Al_2O_3 matrix grains or at grain boundaries [14-17, 25, 26]. Thus, it can be said that the transport properties of alumina/YAG composites the can be related for ionic conductivity, which derived from aluminum ions or oxygen vacancies [20, 21, 24]. At lower volume fraction of YAG particles, the electrical conductivity (Tab. IV) increased slowly with the volume fraction of YAG up to 21 vol%. With further increase of YAG up to 28 vol%, the electrical conductivity of the composites was comparable to that of the pure

alumina. Thus, the presented results indicated that at low YAG contents the particles were not interconnected to form a continuous conductive path.

Tab. IV The electrical conductivity of grain (κ_g) and grain boundary (κ_{gb}) of the alumina/YAG composite.

T (°C)	AY7_1550		AY14_1550		AY21_1550		AY28_1550	
	κ_g $(\Omega^{-1}cm^{-1})$	κ_{gb} $(\Omega^{-1}cm^{-1})$	κ_g $(\Omega^{-1}cm^{-1})$	κ_{gb} $(\Omega^{-1}cm^{-1})$	κ_g $(\Omega^{-1}cm^{-1})$	κ_{gb} $(\Omega^{-1}cm^{-1})$	κ_g $(\Omega^{-1}cm^{-1})$	κ_{gb} $(\Omega^{-1}cm^{-1})$
500	0.82×10^{-3}	1.54×10^{-4}	1.32×10^{-3}	3.44×10^{-4}	2.48×10^{-3}	1.86×10^{-3}	7.88×10^{-5}	9.99×10^{-6}
550	2.03×10^{-3}	4.62×10^{-4}	2.56×10^{-3}	7.78×10^{-4}	3.66×10^{-3}	2.66×10^{-3}	1.87×10^{-4}	3.12×10^{-5}
600	2.66×10^{-3}	5.10×10^{-4}	5.47×10^{-3}	2.26×10^{-3}	7.44×10^{-3}	6.33×10^{-3}	2.55×10^{-4}	4.76×10^{-5}
650	3.41×10^{-3}	1.26×10^{-4}	5.89×10^{-3}	2.76×10^{-3}	1.68×10^{-2}	8.27×10^{-3}	3.02×10^{-4}	6.89×10^{-5}
700	4.65×10^{-3}	2.55×10^{-4}	6.15×10^{-3}	2.98×10^{-3}	2.22×10^{-2}	9.44×10^{-3}	3.44×10^{-4}	8.67×10^{-5}

According to the results of total electrical conductivity (κ) of composite AY21_1550 listed in Tab. IV, the plot logκ=f(1/T) as found and is presented in Fig. 7. Activation energies (Ea) were calculated from Arrhenius plots according to the derived equation $\ln(\kappa T)=\ln A-E_a/k*1/T$ where κ is the conductivity, *T* is the absolute temperature, *A* is the pre–exponential factor and *k* is the Boltzmann constant. Based on studies of different authors and literature data [3, 4], it can be concluded that the value of E_a presented in our work is very lower in comparison with the activation energies for similar conductors [13, 19, 22-24]. This is probably a consequence of well–ordered structure and better processing of obtained powders, which allows easier activation of conductivity carriers and resulting in a decrease of E_a.

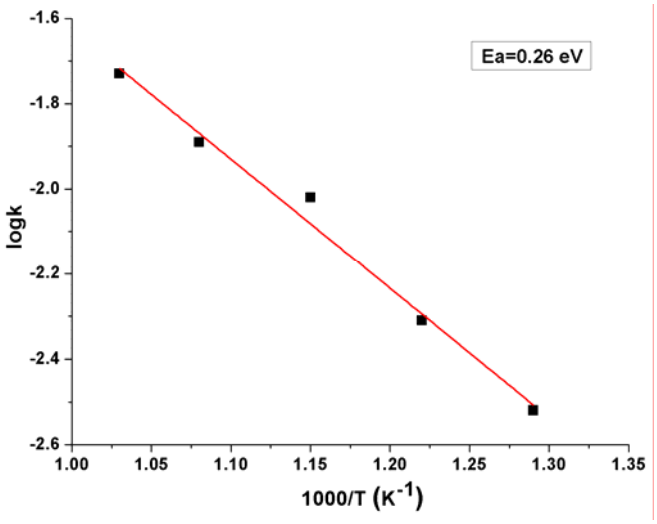

Fig. 7. The dependence-of plot *logk = f(1/T)* of the alumina/YAG composite AY21_1550.

4. Conclusions

The alumina/YAG composites with high relative density were successfully obtained by mixing commercial alumina powder with different volume fraction of yttrium aluminum garnet ($Y_3Al_5O_{12}$-YAG; 7, 14, 21 and 28) synthesized by nitrate-glycine reaction. Polycrystalline YAG powder was obtained by calcination at 950 °C for 2 h. Using XRPD analysis it was found that the particle size of YAG powders lies in the nanometric range, being lower than 35 nm. The high relative density was achieved by compacting at 100 MPa, followed by isostatic pressing with 300 MPa, and then sintering at 1550 °C in the air during different times (2, 4, 6 and 8 h). The achieved highest density was 99.2 % of theoretical density. A significant influence of volume fraction of YAG on formation of a conductive path consisting of mutually interconnected YAG particles was confirmed by SEM microphotographs. In this case, the ionic conductivity is enabled thanks to the transport properties in YAG particles, where the aluminum ions or oxygen vacancies are the carriers of conductive path. The highest electrical conductivity of grain (κ_g) and grain boundary (κ_{gb}) at 700 ºC was 2.22×10^{-2} $\Omega^{-1}cm^{-1}$and 9.44×10^{-3} $\Omega^{-1}cm^{-1}$, respectively was measured in the composites containing 21 vol% of YAG. Based on the obtained results for electrical conductivity, high density and thermal stability, it could be concluded that ceramics material based on Al_2O_3 with different content of second phase may have possible application in IT–SOFC.

5. References

1. Wain-Martin, A. Morán-Ruiz, K. Vidal, A. Larrañaga, M. A. Laguna-Bercero, M. I. Arriortua, Scalable synthetic method for SOFC compounds, Solid State Ionics, 313 (2017) 52-57.
2. Zia Ud Din, Z. A. Zainal, Biomass integrated gasification–SOFC systems: Technology overview, Renewable and Sustainable Energy Reviews 53 (2016) 1356-1376.
3. M. Stojmenović, M. Žunić, J. Gulicovski, D. Bajuk–Bogdanović, I. Holclajtner–Antunović, V. Dodevski, S. Menus, Structural, morphological, and electrical properties of doped ceria as a solid electrolyte for intermediate–temperature solid oxide fuel cells, J. Mater. Sci. 50 (2015) 3781-3794.
4. M. Stojmenović, M. Žunić, J. Gulicovski, V. Dodevski, M. Prekajski, A. Radulović, S. Menus, Structural, morphological and electrical properties of $Ce_{1-x}Ru_xO_{2-\delta}$ (x=0.005-0.02) solid solutions, Ceramics International, 42 (2016) 14011-14020.
5. X. J. Chen, K. A. Khor, S. H. Chan, L. G. Yu, Preparation yttria-stabilized zirconia electrolyte by spark - plasma sintering, Mater. Sci. Eng., A 341 (2003) 43-48.
6. R. Lach, K. Haberko, M.M. Bućko, M. Szumera, G. Grabowski, "Ceramic matrix composites in the alumina/5–30 vol.% YAG system", Journal of the European Ceramic Society 31 (2011) 1889-1895.
7. S. A. Hassanzadeh-Tabrizi, E. Taheri-Nassaj, H. Sarpoolaky, "Synthesis of an alumina–YAG nanopowder via sol–gel method", Journal of Alloys and Compounds, 456 (2008) 282-285.
8. W. Q. Li, L. Gao, "Processing, microstructure and mechanical properties of 25% YAG- Al_2O_3 nanocomposites" Nanostructured Materials, Vol. 11, No. 8, (1999) 1073-1080.
9. A. Egelja, J. Majstorović, N. Vuković, M. Stanković, D. Bučevac, "Synthesis of higly porous Al_2O- $Y_3Al_5O_{12}$ composite ceramics ", Science of sintering, 48 (2016) 303-315.

10. J. Alkebro, S. Begin-Colin, A. Mocellin, R. Warren, "Mechanical alloying of alumina-yttria powder mixture", Journal of the European Ceramic Society, 20 (2000) 2169-2174.
11. H. Wang, L. Gao, "Preparation and microstructure of polycrystalline Al_2O_3- $Y_3Al_5O_{12}$ composites", Cheramics International, 27 (2001) 721-723.
12. S. Ramanathan, M. B. Kakade, S. K. Roy, K. K. Kutty, "Processing and characterization of combustion synthesized YAG powders", Ceramics International, 29 (2003) 477-484.
13. M. Parchovianský, D. Galusek, P. Švančárek, J. Sedláček, P. Šajgalík, Thermal behavior, electrical conductivity and microstructure of hot pressed Al_2O_3/SiC nanocomposites, Ceramics International, 40 (2014) 14421-14429.
14. V. V. Mitic, V. Paunovic, J. Purenovic, S. Jankovic, L. Kocic, I. Antolovic, D. Rancic, The contribution of fractal nature to $BaTiO_3$-ceramics microstructure analysis, Ceramics International, 38 (2012) 1295-1301.
15. V. V. Mitic, V. Paunovic, L. Kocic, Fractal approach to $BaTiO_3$-ceramics micro-impedances", Ceramics International, 41 (2015) 6566-6574.
16. V. V. Mitic, L. Kocic, V. Paunovic, F. Bastić, D. Sirmić, The fractal nature materials microstructure influence on electrochemical energy sources, Science of Sintering, 47 (2015) 195-204.
17. V. V. Mitić, Lj. M. Kocić, S. Tidrow, H.-J. Fecht, Structures, Fractals and Energy, In: Nanotechnology for Energy Sustainability, 2 Vol., pp. 781-808 (Baldev Raj, Marcel Van de Vorde, Yashwant Mahajan eds.), Wiley-VCH Verlag GmbH&Co KgaA, Weinheim, Germany 2017.
18. D. Stauffer, A. Aharony, Introductionto Percolation Theory, London 1992.
19. D. S. McLachlan, M. Blaszkiewitz, R. E. Newnham, J. Am. Ceram. Soc., 73 (1990) 2187-2203.
20. S. R. Rotman, H. L. Tuller, Ionic Conduction in Yttrium Aluminium Garnet, Solid State lonics, 40/41 (1990) 893-895.
21. L. Schuh, R. Metselaar, Computer Modelling Studies of Defect Structures and Migration Mechanisms in Yttrium Aluminium Garnet, J. Eur. Ceram. Soc., 7 (1991) 67-74.
22. J. L. Bates and J. E. Garnier, Electrical conductivity of MgAl/sub 2/O/sub 4/ and Y/sub 3/Al/sub 5/O/sub 12/, J. Am. Ceram. Soc., 64 (1981) C–138.
23. A. Y. Neiman, E. V. Tkachenko, and V. M. Zhukovskii, Defect formation in complex oxides of composition R sub 3 sup III E sub 5 sup III O sub 12 with the garnet structure, (R= rare earths and Y; E= Al, Ga, Fe), Dokl. Akad. Nauk SSSR, 240 (1978) 876.
24. L. Schuh, R. Metselaar, and G. de With, Microstructure and defect chemistry of yttrium aluminium garnet ceramics, J. Appl. Phys., 66 (1989) 2627.
25. R. Waster, R. Hagenbeck, Grain boundaries in dielectric and mixed - conducting ceramics, Acta Mater. 48 (2000) 797-825.
26. S. H. Jensen, A. Hauch, P. V. Hendriksen, M. Mogensen, N. Bonanos, T. Jacobsen, A Method to Separate Process Contributions in Impedance Spectra by Variation of Test Conditions, J. Electrochem. Soc. 154 (2007) B1325-B1330.

Садржај: *Алумина/YAG композити (AYX_t) са високом релативном густином (99,2 %TD) су успешно добијени мешањем комерцијалног праха алуминијума са различитим запреминским фракцијама итриум алуминијског граната ($Y_3Al_5O_{12}$-YAG; 7, 14, 21 и 28). У облику прашка прекурсора YAG је синтетисан глицин нитратном реакцијом. Поликристални YAG прах добијен је калцинацијом на 950 °C током 2 h. Даље, добијене композиције у облику праха (AYX_p) су компактиране на 100 MPa, изостатски*

пресоване на 300 MPa и затим синтероване на 1550 °C у ваздушној атмосфери током различитих временских периода (2, 4, 6 и 8 h). Поред тога, добијене композиције су карактерисане XRD, SEM, EDX и електрохемијском импеданчном спектроскопијом. XRD анализа је показала да величина честица YAG праха лежи у нанометријском опсегу (мања од 35 nm). SEM микрофотографијама композита потврђено је формирање проводне стезе састављене од међусобно повезаних честица YAG. У овом случају, јонска проводљивост је омогућена захваљујући својствима транспорта у YAG честицама, где су јони алуминијума или кисеоничне ваканције носиоци проводне путање. То је потврђено електрохемијском импеденцијалном спектроскопијом. Највећа електрична проводљивост зрна (κ_g) и граница зрна (κ_{gb}) на 700 ºC износила је 2.22×10^{-2} $\Omega^{-1}cm^{-1}$and 9.44×10^{-3} $\Omega^{-1}cm^{-1}$, респективно, мерена је у композиту који садржи 21 vol% YAG. На основу добијених резултата може се закључити да керамички материјал заснован на Al_2O_3 са садржајем друге фазе може имати могућност примене у IT–SOFC.

Кључне речи: *Al_2O_3-YAG; композити; електрична проводљивост.*